American Society of Mechanical Engineers

ASME SETTING THE STANDARD

ASME Accepted Manuscript Repository

titutional Repository Cover Sheet

Cranfield Collection of E-Research - CERES

ASME Paper Tile: Injector Design Space Exploration for an Ultra-Low NOx Hydrogen Micromix Combustion System

Authors: Parash Agarwal, Xiaoxiao Sun, Pierre Q. Gauthier, Vishal Sethi

ASME Conference Title: Proceedings of ASME Turbo Expo 2019: Turbomachinery Technical Conference and Exposition

Volume/Issue: Volume 3 Date of Publication (VOR* Online) 5 November 2019

ASME Digital Collection URL: https://asmedigitalcollection.asme.org/GT/proceedings/GT2019/58608/V003T03A013/1066673

DOI: 10.1115/GT2019-90833

*VOR (version of record)

Proceedings of ASME Turbo Expo 2019:
Turbomachinery Technical Conference and Exposition
GT2019
June 17-21, 2019, Phoenix, Arizona, USA

GT2019-90833

INJECTOR DESIGN SPACE EXPLORATION FOR AN ULTRA-LOW NO_X HYDROGEN MICROMIX COMBUSTION SYSTEM

Parash Agarwal*
PhD Researcher
SATM Cranfield University
Cranfield, Bedfordshire, UK
Email: p.agarwal@cranfield.ac.uk

Xiaoxiao Sun
PhD Researcher
SATM Cranfield University
Cranfield, Bedfordshire, UK
Email: x.sun@cranfield.ac.uk

Dr Pierre Q. Gauthier
Royal Academy of Engineering Visiting Professor
in Low Emissions Combustion System Modelling
SATM Cranfield University
Cranfield, Bedfordshire, UK
Email: p.gauthier@cranfield.ac.uk

Dr Vishal Sethi
Senior Lecturer in Gas Turbine Combustion
and Environmental Impact
SATM Cranfield University
Cranfield, Bedfordshire, UK
Email: v.sethi@cranfield.ac.uk

ABSTRACT

The depletion of fossil fuel resources, as well as the increasing environmental concerns have become the driving forces towards the research and development necessary for the introduction of alternative fuel such as hydrogen into civil aviation. Hydrogen is a suitable energy source primarily because it is free of carbon and other forms of impurities and is also the most abundant element in the universe. The advantages of using Liquid Hydrogen (LH_2) for civil aviation extends beyond carbon-free mission level emissions; LH_2 combustion can potentially reduce NO_x emission by up to 90%, providing long-term sustainability and unrivalled environmental benefits.

The paper presents a simplified parametric analysis to investigate the influence of various injector design parameters on a hydrogen micromix combustor reactive flow field. The main characteristics investigated are the flame structure (shape and position), the aerodynamic stabilization of the flame and the resulting NO_x emissions. The design parameters include variations in the air-feed dimensions and the hydrogen injection diameter. A suitable numerical model was established by comparing various turbulence modelling approaches, reaction mechanisms and turbulence-chemistry interaction modelling schemes. The predictive capabilities, and limitations, of each of these modelling approaches, are assessed. The numerical challenges and limitations associated with modelling H_2/air combustion at high pressure and temperature conditions are detailed. The influence of varying the injector design parameters on the mixing and hence the NO_x characteristics is assessed.

NOMENCLATURE

Acronyms	
AGP	Air Guiding Panel
BR	Blockage Ratio
CFD	Computational Fluid Dynamics
DOE	Design of Experiments
ENABLEH2	ENABLing cryogenic Hydrogen based CO2-free air transport
FGM	Flamelet Generated Manifold
H_2	Molecular Hydrogen
LBV	Laminar Burning Velocity (m/s)
LES	Large Eddy Simulations
LH_2	Liquid Hydrogen
NO_x	Nitrogen Oxides
OH	Hydroxyl Radicals
PDF	Probability Density Function
RANS	Reynolds- Averaged Navier Stokes Equations
TRL	Technology Readiness Level
Symbols	
J	Momentum Flux Ratio
d	Diameter (mm)
u	Velocity (m/s)
ρ	Density(kg/m^3)
∞	Free Stream
Φ	Equivalence Ratio

*Address all correspondence to this author

Copyright © 2019 ASME
Published by The American Society of Mechanical Engineers. This is the Author Accepted Manuscript issued with:
Creative Commons Attribution License (CC BY). The final published version is available online at DOI: 10.1115/GT2019-90833.
Please refer to any applicable publisher terms of use.

INTRODUCTION

The continued growth of the aviation industry, combined with growing environmental concerns and the depletion of the fossil fuel resources makes it is necessary to develop clean and efficient technologies for a sustainable growth in aviation.

The total consumption of aviation fuel was estimated to be 6.8 million barrels a day in 2007 [1]. Currently, the aviation fuel constitutes about 6% of the oil consumption globally. This accounts for about 2.1% of total anthropogenic CO_2 emissions or 12% of the total carbon emissions from all transport sources [2]. Aircraft NO_x emissions contribute about 75-80% of the total airport NO_x emissions. These figures are for the year 2016, however, IATA projects an increase in air traffic by about 3-5% a year for the passenger transport sector and about 9-10% for the cargo sector over the next 20 years [3].

To curb the environmental impact of the aviation industry, ambitious targets have been set by flightpath 2050 which includes 75% reduction in CO_2 emission per passage kilometre, 90% reduction in NO_x emissions and 65% reduction in perceived noise emission relative to the year 2000 technologies [4]. However, increasing evidence suggests that these targets would be very challenging to meet with conventional carbon-containing fuels, despite the large research efforts ongoing for airframe, propulsion technologies and improved asset management. LH_2 as a fuel provides an alternative to meet these highly ambitious targets.

The emissions resulting from LH_2–fueled combustion systems differ significantly from hydrocarbon combustion. LH_2 combustion does not produce any carbon pollutant species, in fact, the primary combustion products from hydrogen combustion is the formattion of water vapour. Water vapour is also considered a greenhouse emission however, unlike hydrocarbons, its effect depends upon the altitude of the cirrus cloud formation. Moreover, the residence time of water vapour is relatively short; several days or up to one year [5][6].

The thermodynamic cycle of a gas turbine engine demands that he combustion processes take place at relatively high levels of temperature, which favour the formation of NO_x. The combustion of LH_2 as a fuel has a greater potential to generate higher NO_x than conventional kerosene fuel primarily because of its higher flame temperature at a given equivalence ratio (Φ). However, since LH_2 has a wider flammability limit, the entire combustion zone can be made significantly leaner, resulting in lower flame temperatures and hence reduced NO_x emissions. Figure 1 presents the flame temperature for hydrogen and kerosene as a function of the combustor primary zone Φ.

Premixing of an LH_2 combustor would, therefore, be very desirable from the low-NO_x prospective. However, obtaining primary zone Φ uniformly low enough to inhibit excessive NO_x values is quite challenging; imperfections in the fuel/air mixing can potentially lead to local rich fuel-air pockets, leading to a greater presence of hot spots and corresponding peaks in NO_x production. Another issue that can potentially arise with a premixed system is the enhanced risk of autoignition and flashback due to the high reactivity of LH_2-air mixtures [8]. The high stoichiometric temperature, and the high reactivity associated with hydrogen, therefore makes it imperative to have the necessary methods and tools available for the design fuel injection systems that can ensure good mixture homogeneity while, at the same time, mitigating the risks associated with autoignition and flashback.

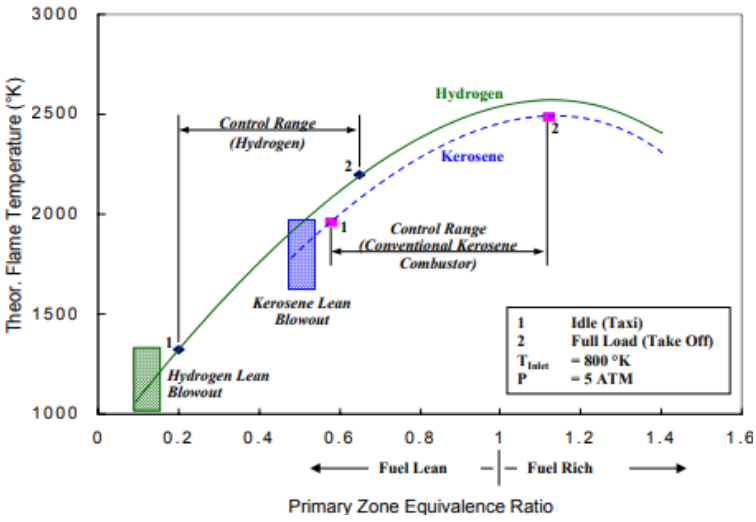


Figure 1- Temperature Characteristics [7]

Although the uptake of LH_2 for aviation is still in its infancy, it can be assumed that the LH_2 will play a vital role in alleviating environmental impact of the aviation. It is therefore vital to develop both the analytical and experimental tools to further mature the technologies to higher TRL levels for the use of LH_2 for civil aviation. The micromix combustion principle has been investigated at Cranfield University over the past years [9-15]. The scope of the current work will feed into the research and innovation efforts by Cranfield University as a part of the ENABLEH2 project [19]. This involves the design and development of a novel ultra-low-NO_x micromix combustor system to TRL levels 3-4.

The present study outlines the preliminary numerical methodology adopted to explore the design space and the reactive flow fields associated with micromix combustion. The study has been subdivided into two parts. The first part involves a turbulence-chemistry interaction modelling study using three different reduced hydrogen chemistry mechanisms, at high pressure and temperature condition. The applicability and predictive capabilities of each of these mechanisms are analysed to down-select the best candidate for further parametric analysis. The second part of this study involves a preliminary parametric analysis. As a part of this parametric study the influence of varying the air feed hydraulic diameter and the hydrogen inlet diameter on the reactive flow field, and hence the flame aerodynamic stability is analysed.

Copyright © 2019 ASME

Micromix Combustion Concept

The combustion characteristics of hydrogen differ significantly from that of kerosene as stated above. Therefore, to ensure good mixing homogeneity and to avoid issues associated with flashback and autoignition, the concept of "micromix combustion" was conceived by the FHA Aachen University [8]. The micromix combustion concept can be characterised as an method to, "minimise the scale of mixing but to increase the mixing intensity" [8]. The mixing of the fuel and air in the local zone is significantly increased compared to conventional gas turbine combustor designs. This maximising of the mixing intensity is however limited by the maximum pressure loss of modern gas turbine combustor designs, which should not typically exceed 3-4% [8].

The mixing process in a micromix system is significantly improved by the principle of the jet-in-cross-flow. The flame anchoring, which is essential for the reduction in NO_x formation, is achieved primarily by the recirculation vortices and by the momentum flux ratio of the crossflow streams[63] [17]. The conceptual micromix combustor design conceived at Cranfield University is shown as in Figure 2.

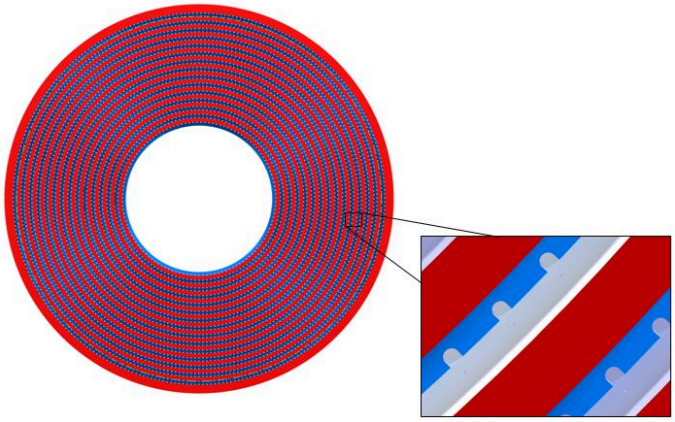


Figure 2 - Schematic front view of the Micromix Annular Burner Segment

Micromix Design Parameters

The geometrical parameters for this micromix combustion design are essential to ensure the right penetration depth of hydrogen into the oncoming airstream. A single injector arrangement is shown as in Figure 3. The air stream flows through the micromix structure from left to right direction. The hydrogen jet penetrates perpendicular to the air stream shown in Figure 3. The turbulent generation and resulting eddy break down rapidly mixes the stoichiometric combustion zones formed locally of these micro-diffusion flames, hence reducing the local residence time at high-temperatures, and subsequent thermal NO_x formation [16].

Recirculation vortices are required to anchor, stabilise and position the micro-flames over a range of engine operating conditions. The flames shape, size and position can then be adjusted by modifying the location and size of the recirculation zones downstream the micromix injector array. The presence of these recirculation areas are essential to ensure that the micro-flames are stable and are separated from each other in the vertical direction. It is critical to the design of the micromix system that these micro flames are separated from each other since the merging of adjacent flames could potentially result the formation of larger-scale flames. This would further increase fuel-air mixtures residence time in the hot recirculation regions and subsequently increase the NO_x emissions, while potentially overheating the combustor liner [61].

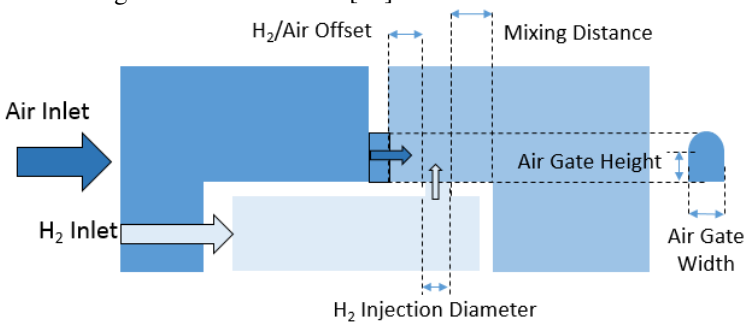


Figure 3- Design Variable for Single Injector Study

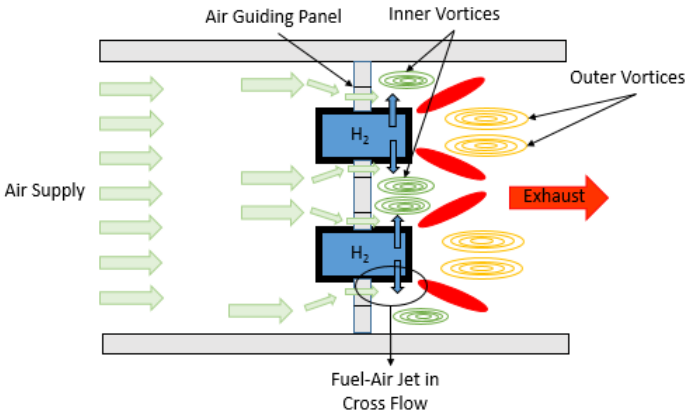


Figure 4- Schema of the Aerodynamic Stabilisation Principle (Image adapted from [17])

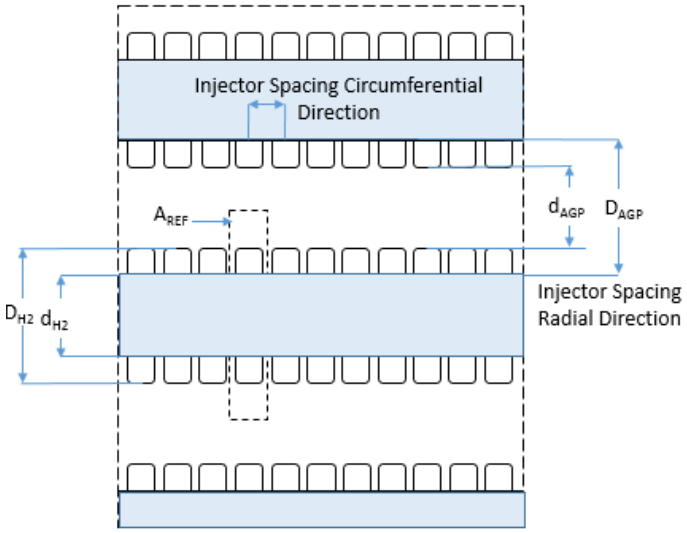


Figure 5- Definition of the Injector Blockage Ratio

Copyright © 2019 ASME

Momentum Flux Ratio

The other main parameter that influences the micromix combustion system design is the momentum flux ratio between the fuel jet and the air crossflow. This momentum flux ratio is defined as [63]:

$$J = \frac{\rho_j * u_j^2}{\rho_\infty * u_\infty^2} \qquad (3)$$

Increasing the momentum flux ratio between the two streams increases the penetration depth of the hydrogen stream into the jet-in-cross-flow air stream thus enhancing the mixing characteristics [61][63]. The air stream jet air mixes with the penetrating hydrogen stream, the inner recirculation zones are then divided by shear layers between the two streams. If the penetration depth is below a critical penetration height, the H_2-air mixture can be discharged freely, and the residence time is short. If, however, the penetration depth increases beyond this critical value, the hydrogen penetrates the shear layer between the two streams and hence enters into a hot inner recirculation zone [63], as shown in Figure 6. This further increases the residence time of the mixture, subsequently leading to an increase in NO_x emissions [17]. Hence the determination of this critical penetration depth (y_{crit}) is of vital importance to the design of the micromix system. The penetration depth and momentum flux ratio is dependent by equation (4):

$$y_{H2} \propto d_{H2} \times \sqrt{J} \qquad (4)$$

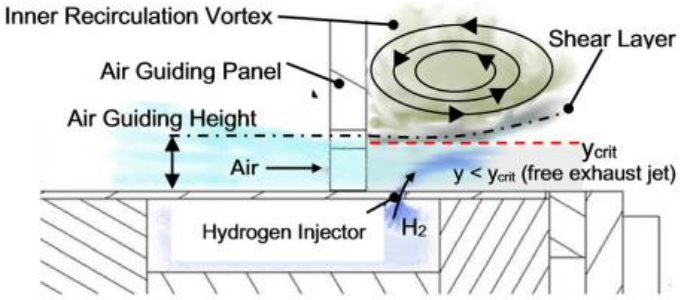


Figure 6- Hydrogen Penetration Depth Definition [17]

Numerical Analysis

For the initial simulations of a single injector, a simplified numerical model of the geometry was solved for using ANSYS FLUENT™. A 3D numerical model of the micromix combustor section was created to analyse the reactive flow field using a RANS based solver along with a detailed H_2/air reaction mechanism and a thermal NO_x formation model. The resulting flow fields, temperature profiles, and OH species distribution across the computational domain were analysed. The influence of various geometrical design parameters on flame anchoring, its structure and hence the resulting emissions behaviour were also analysed. The aim of this preliminary numerical analysis was to understand the reacting flow characteristics of the jet-in-crossflow configuration and also to qualitatively identify the tendencies of varying injector designs. The analysis carried out as a part of this work would be used to inform and guide the design of the experimental rig to be developed as a part of the ENABLEH2 project at Cranfield [12]. More details of the numerical model used for this study are stated below.

Computation Domain

The geometrical model of a single injector used this study is shown in Figure 11. It covers a longitudinal slice of a single injector configuration. It consists of an air inlet upstream of the burner geometry, the hydrogen inlet perpendicular to the air stream and the combustion volume.

Adiabatic wall with no-slip boundary conditions are initially used, instead of a symmetry boundary condition. This is done to isolate the effects of injector-injector interactions. The hydrogen and the air are injected through two discrete streams. The spatial discretisation of the computational domain consists of approximately 2.1 million hexahedral elements. The Φ used for this numerical study is assumed to be 0.43, an assumption based on the previous analysis carried out by Aachen [21]. A detailed analysis on the effect of varying Φ on the hydrodynamic instability characteristics of this concept is required to derive the lean limit of hydrogen combustion at a given temperature and pressure condition and will be carried out in future work. The mass flow rate of the hydrogen is determined by the heat release required by each of the injectors for the micromix system. For the purposes of this study, the heat release per injector is assumed to be 3.74 kW and is kept constant. The combustor performance data and the boundary conditions imposed at the air and fuel inlet ports are summarised in Table 1. The fuel and air inlet boundary conditions used are representative of a typical ultra-high bypass ratio engine configuration for entry into service by the year 2050. The 3D steady RANS calculations have been performed using the *k-ω* SST turbulence scheme. The shear stress transport (SST) formulation allows for integration down to the wall, through the viscous sub-layer, resulting in a more accurate near wall treatment, which is vital for such designs involving small geometric features. This is particularly important when required to accurately capture a broad spectrum of eddies, ranging all the way from smaller scales of eddies in the hydrogen jet to the larger eddies in the recirculation zones [22].

Table 1: Simulation Boundary Conditions

Boundary	Parameter	Value
Air Inlet	Temperature (K)	860
	Mass Flow (kg/s)	1.9E-03
Hydrogen Inlet	Temperature (K)	300
	Mass Flow (kg/s)	2.0E-05
Combustor Inlet	Pressure (MPa)	2.046
	Temperature (K)	860
Combustor Outlet	Temperature (K)	1540

Copyright © 2019 ASME

The primary challenges associated with turbulence chemistry modelling is to resolve the turbulent mixing scales along with combustion chemistry. This may involve solving hundreds of molecular species, in a solution time compatible with the engineering design cycle time [23]. Hence, the combustion reaction kinetics for the present work are modelled using the FGM approach for a partially premixed diffusion flamelets [24][25]. FGM is an industry standard approach used to reduce the computational expenses associated with directly solving the reaction kinetics. The FGM modelling approach is based on the fact that in many combustion processes, the chemical, or reaction time scales occur much faster than the actual flow time scales. These fast chemical processes can therefore be decoupled. This reduces the stiffness of the numerical model and therefore reduces the computational costs [24]. The turbulent flame is assumed to be an ensemble of laminar flames, the internal structure of which is not significantly influenced by the flow turbulence. These flamelets are then embedded into the turbulent flame brush using statistical averaging. The species and associated thermodynamics are parameterised by just a few variables such as reaction progress, scalar-dissipation and mixture fraction. A set of transport equations are then solved for these variables. FGM is fundamentally different from other laminar flamelet models primarily because of its capability to model non-equilibrium effects. Since these other laminar flamelets models are parameterised by strain, the thermochemistry always tends to equilibrium as the strain rate decays towards the exit of the combustor. In contrast, the FGM model is parameterised by the reaction progress variable; therefore, the flame can be fully quenched. No assumptions of thin and intact flamelets are made by the FGM. This is particularly important when modelling ignition and extinction phenomenon. The flamelet library is created using the ANSYS FLUENT 19.1 diffusion laminar flamelet generator [25]. Many works exist in the literature stating the limitations, the applicability and the predictive capabilities of using FGM to model the combustion reaction kinetics [25-27] [60].

The default number of flamelets that can be generated has been capped to 100 in ANSYS FLUENT. Due, to the high pressure and temperature conditions for the present numerical simulations, the original set of hydrogen flamelets were observed to be extinguished at a strain rate of 7851/s, and a scalar dissipation increment of 79/s had to be used to respect the default number of flamelets. However, such high scalar dissipation step may lead to poor interpolation within the PDF lookup table and therefore affect the predictive capabilities of the combustion kinetics. To reduce the scalar dissipation step size to a more reasonable size, a scheme has been developed and implemented in a FLUENT to increase the default number of flamelets to 1600. Scheme is a LISP dialect used to develop the Fluent GUI, and is often used to interact with the FLUENT journal files via parameters. By the implementation of scheme the scalar dissipation steps can be reduced to 5/s, allowing for a much finer discretisation of the flamelet space.

The kinetics of the thermal NO_x formation rate is much slower than the compared to the energy-releasing reactions, and so most of the thermal NO_x is formed only after the complete combustion. Theoretically, the FGM modelling approach can be used to simulate the slow chemistry of NO_x formation but the degree of uncertainty associated with it is very high [24]. For the purposes of this analysis, the thermal NO_x predictions are estimated, in a post-processing exercise, using the extended Zeldovich mechanism on the frozen reactive flow field predicted by the FGM model.

Combustion Reaction Mechanism Comparison

There are several mechanisms available in the literature for hydrogen combustion. Each of these mechanisms has been developed under varying experimental types and conditions. Carsten [28] has carried out a comprehensive comparison of the published hydrogen combustion mechanisms. For the purposes of this study three mechanisms have been down-selected based on previous work carried out at Cranfield [29]. The previous work at Cranfield was limited to the analysis under atmospheric pressure conditions only. It is known that although hydrogen has a relatively simple reaction mechanism, the mechanism is also highly dependent on the pressure conditions. Therefore, the down selection of hydrogen-air mechanisms under high-pressure conditions was carried out. The manifold represents the chemistry inside a three-dimensional CFD simulation. The turbulence-chemistry interaction is pre-tabulated for the entire manifold and therefore requires no added computational efforts. This enables the use of detailed combustion chemistry mechanism with no added computational costs.

Although various mechanisms are available in the literature [30-48], there are relatively very few mechanisms that have been derived under high-pressure experimental conditions. The mechanisms analysed are shown in Table 2.

Table 2 List of the Combustion Kinetics Mechanisms Used

Mechanism ID	Ref	Species Number	Reaction Number
Naik	[50]	9	25
GRI-Mech 3.0	[43]	53	325
DRM 1.2	[49]	22	104

GRI-Mech 3.0 [43] is used in various industrial applications for simulations and it covers hydrogen and many hydrocarbon combustion reactions. DRM 1.2 [49] was developed as a truncated version of the GRI-Mech. This was done to develop a smaller subset of reactions capable of closely producing the main combustion characteristics as predicted by the complete mechanism. CV Naik [50] mechanism, on the other hand, is developed to simulate the combustion of pure H_2 and O_2 mixture, over wider range of pressure ranging from 0.05 atm to 87 atm, Φ from 0.2 to 6 and temperatures ranging from 298K to 2700K.

Copyright © 2019 ASME

Laminar Burning Velocity

Laminar burning velocity is considered to be among the most important combustion parameters used in assessing many phenomena like ignition, quenching of the flame, and its flashback stabilisation [51]. LBV *vs* Φ of the mechanisms is shown as in Figure 7. Laminar burning velocity of an H_2 and air mixture is generally much higher than for conventional fuels, an outcome associated with the high reactivity of H_2/air. Generally, the same laminar burning velocity is predicted by all the three mechanisms, over a wide range of Φ as shown in Figure 7.

However, at very high values of Φ (>5) and high-pressure conditions, the GRI-Mech 3.0 tends to overpredict the laminar burning velocity by about 40-50 % compared to the other two mechanisms as shown in Table 3. Such variations are observed at very lean conditions as well. Similar discrepancies have been reported under lean high-pressure conditions by Goswami [59] where the researcher concluded the unsuitability of using the GRI-Mech3.0 mechanism for pure hydrogen combustion under such high pressure and lean conditions.

Table 3: Equivalence Ratio vs Laminar Burning Velocity

Mechanism	Equivalence Ratio	Laminar Burning Velocity (m/s)
Naik [50]	0.205	1.78E-05
	1.00	8.89E+0
	5.24	3.75E-06
GRI-Mech 3.0 [43]	0.205	1.15E-05
	1.00	8.79E+0
	5.24	5.43E-06
DRM 1.2 [49]	0.205	1.73E-05
	1.00	8.85E+0
	5.24	3.58E-06

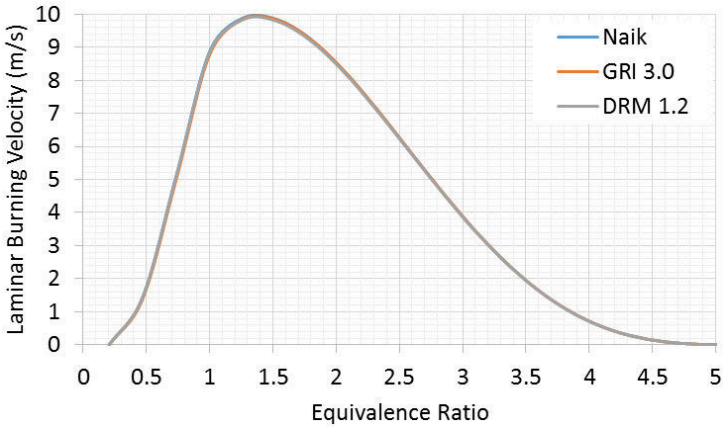


Figure 7- Laminar Burning Velocity vs Equivalence Ratio

OH Radical Distribution

The concentration of OH species is of prime importance in a hydrogen combustion system and is often employed as a flame marker. Among the various reaction steps one of the most important chain propagation reaction steps of hydrogen reaction, and in NO_x chemistry, is the reaction between the molecular oxygen and hydrogen radical to form hydroxyl and oxygen radicals ($H + O_2 = OH + O$) and the reaction of an oxygen radical with molecular hydrogen to form hydrogen and hydroxyl radical ($O + H_2 = OH + H$). The reaction rate coefficients of these reaction steps are highly dependent on the conditions under which the experimental analysis was carried out [53]. Large number of experimental analysis have been carried out to determine the rate constants of this specific reaction step; literature [53] suggests that significant disagreement still prevails in their determination. The OH species distribution along the computational domain is shown as in Figure 8. The variations of OH radicals predicted by each of these mechanisms can perhaps be attributed to the experimental conditions under which the reaction rate constants were determined.

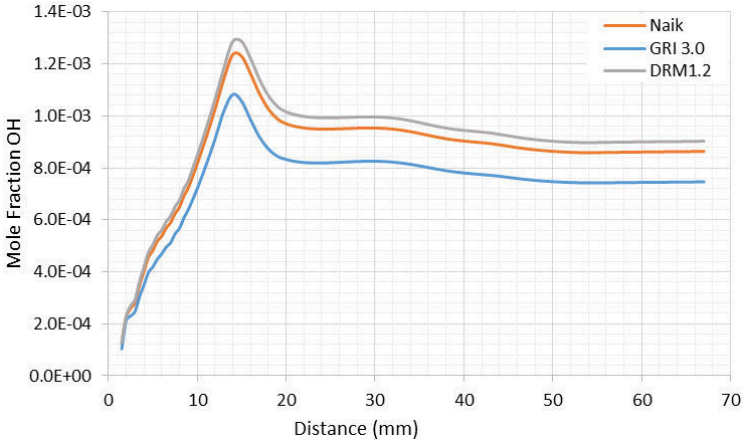


Figure 8- Area Weighted OH Mole Fraction along the Computational Domain

Temperature Distribution

The mass-weighted temperature distribution along the mid-section of the computational domain is shown in Figure 9. All the three mechanisms tend to follow the same temperature trend across the domain. However, upon closer analysis, the peak temperatures predicted by these mechanisms show important variations with peak temperatures of 2648 K, 2603 K and 2545 K predicted by DRM 1.2, Naik, and GRI-Mech3.0 respectively. This may be attributed to variations in the formation of the OH radical predicted in the reacting domain, since the same trends observed for the peak temperature distributions are also observed for the OH radical distributions. The formation of OH radical in the hydrogen reacting system is an exothermic reaction process. The discrepancies in the prediction of hydroxyl radicals can, therefore, lead to variations in the peak temperature distribution and consequently variations in NO_x chemistry.

Copyright © 2019 ASME

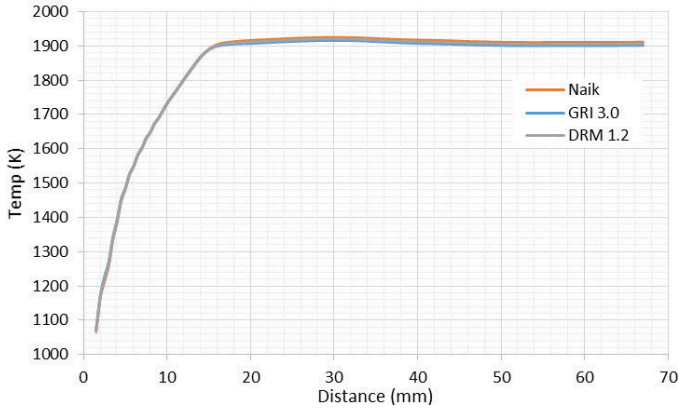


Figure 9- Area Weighted Total Temperature along the Computational Domain

NOx Distribution

The presence of high-temperature peaks will further influence the chemistry of the thermal NO_x formation. In fact, the thermal NO_x formation doubles for every 90K temperature increase beyond 2200 K [54], hence the trends shown in Figure 10. The NO_x values shown in Figure 10 are normalized against the peak area averaged NO_x value predicted by GRI-Mech3.0 mechanism, this is due to the uncertainty in the absolute value of the NO_x emissions predicted by the current numerical model as stated previously.

Both the GRI-Mech3.0 and DRM 1.2 mechanism have been highly optimised for natural gas combustion and perhaps because of this, it fails to predict the hydrogen reaction accurately. In fact, various researchers have questioned the applicability of the GRI-Mech 3.0 for hydrogen combustion [28] [52].

Based on this analysis, the Naik mechanism was down-selected to be used for further analysis. The reasons for the uncertainties associated with these mechanisms are highly debatable and hence require further experimental validation which would be carried out as a part of future work.

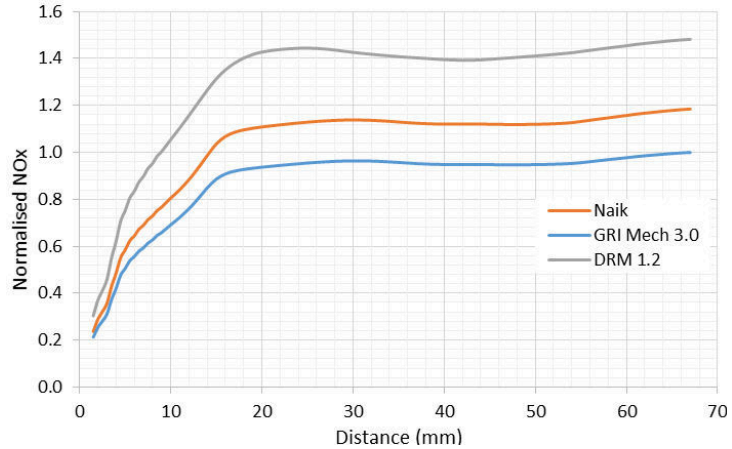


Figure 10 - Normalised NOx distribution along the Computational Domain

The driving design factor of a jet in crossflow is to obtain a homogenous mixture rapidly of the injected fuel and the free stream air. The degree and the rate of the mixing process are important as it affects the combustion process. The burning efficiency and exhaust compositions are directly depend upon the reaction kinetics and mass transfer. The chemical kinetics are difficult to control but, the mixing process is more readily controlled by many numbers of parameters. The flame obtained by the present micromix combustor concept is anchored, near the edge of the hydrogen injector segment, by two recirculation zones and is characterised by two distinct reaction zones, as shown in Figure 4. The outer zone is formed by the recirculation of hot combustion products downstream the H_2 penetration site and the inner zone is formed by the recirculation of the air downstream the air feed panel as shown in Figure 11. Shear layers is established between the two recirculation zones because of the shift in the axial position of the H_2 stream and the reaction zone is established along the inter-recirculation shear layer. The orientation and the structure of these micro-flames are in fact influenced by the shear layer. This shear layer is in turn defined by the size and the position of the recirculation vortices [15].

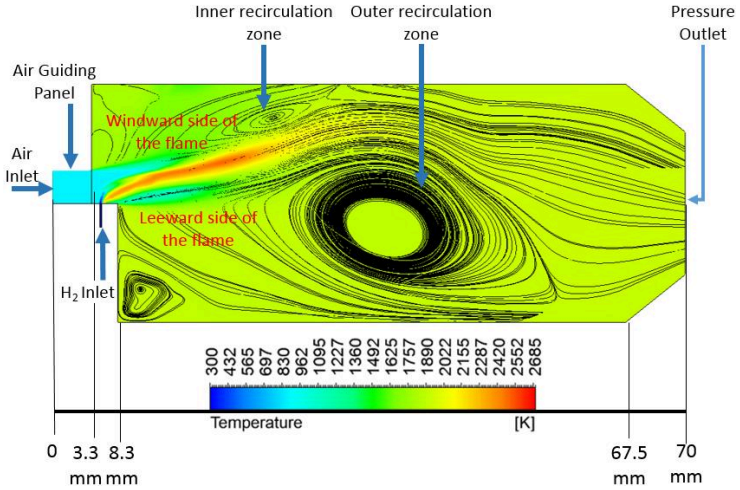


Figure 11- Recirculation and the Vortex Structure of a Micromix Flame

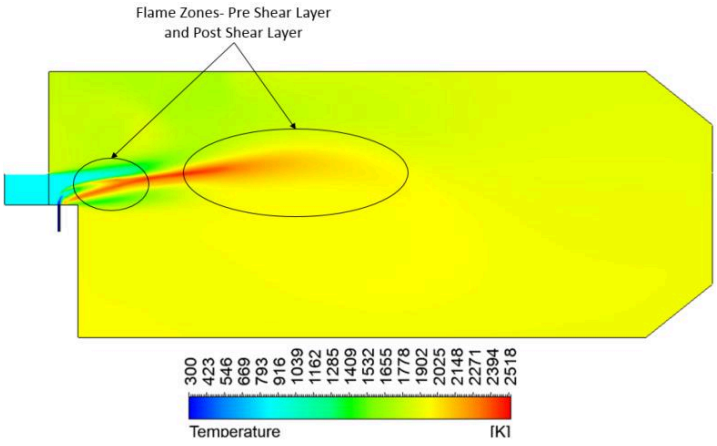


Figure 12: Formation of the Micro-Flame Zones

Copyright © 2019 ASME

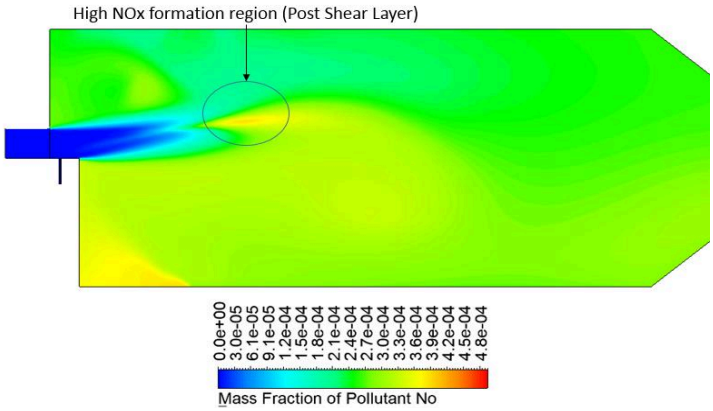


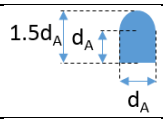
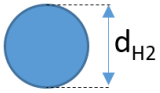
Figure 13- High NO_x Formation Regions

From Figure 12, two distinct temperature zones can be identified. The first flame zone is stabilised between the outer and the inner recirculation zones and hence the formation of the inter recirculation shear layer. The flame region is very thin and shows a high temperature gradient across the flame because of the presence of the reaction zone. The second peak temperature region is identified downstream of the inter-vortex shear layer. Here the remaining unburnt H_2 from the first flame region starts to react. This kind of flame structure isn't typical of a micromix combustor. The micromix principle aims to combust all the injected fuel in the thin inter-vortex shear layer thus avoiding high fuel concentration and, high-temperature peak and consequently reduced NO_x formations [61][62].

Parametric Analysis

The various geometrical parameters that influence the design of the micromix injector are shown in Figure 3. Each of these design variables influence the mixing characteristics between the fuel and oxidiser streams therefore the NO_x emissions. One of the primary factors that influence the design of the micromix system is the momentum flux ratio between the fuel and oxidiser stream. As a part of this study, the influence of varying the air feed panel hydraulic diameter and the hydrogen inlet diameter and their subsequent impact on the momentum flux ratio and NO_x emission characteristics are analyzed. A reference geometry is scaled based on the previous work carried out by Aachen [17], such that the momentum flux ratio was kept constant but with an increased heat release for the current analysis. The reference geometry design parameters are shown in Table 3.

Table 3 : Reference Geometry Design Parameters

	Shape	Hydraulic Diameter (mm)	Aspect Ratio
Air Feed Panel		1.828	1.5
Hydrogen Inlet Diameter		0.5	1

With the reference geometry shown in Table 3 the following parametric studies have been carried out:

1. Variation in the hydrogen inlet diameter: The hydrogen inlet diameter is varied ranging from 0.183 mm to 0.5 mm. The geometrical model is parametrised using ANSYS scripting, such that any variations in the hydrogen inlet diameter would not influence the mixing distance and the offset distance between the hydrogen and the air stream. This is done to isolate the influence of a single parameter variation i.e. the hydrogen inlet diameter on the mixing and hence the emission characteristics.
2. Variations in the air feed panel hydraulic diameter: The air feed hydraulic diameter has been varied ranging from 1.83 mm to 3.34 mm. The aspect ratio of 1.5 for the air feed panel is kept constant for all the analysis. The mixing and the offset distance are both kept constant. The height of the computational domain is scaled proportionally to the variation in the air feed hydraulic diameter, this is done to reduce the impact of hydrogen feed height on outer recirculation zone.

The hydraulic diameter of the air feed panel and the diameter of hydrogen inlet is varied such that the momentum flux ratio ranges from 0.5 to 20.

RESULTS AND DISCUSSION

The influence of varying hydrogen injector diameter on the NO_x distribution is shown in Figure 14. All the measurements for the NO_x emission were taken at plane x=70 mm downstream the injector segment. The location of the measurement plane was selected such that it lies downstream the established mixing region. The plot is normalised using the mass-weighted average NOx predicted at x =70 mm from the reference geometry. From Figure 14 with a decrease in hydrogen inlet diameter, and the associated increase in the momentum flux ratio and mixing characteristics, there is a net improvement in predicted NO_x formation. However, beyond a certain decrease in the hydrogen inlet diameter, the NO_x emissions begin to increase. This can be attributed to the penetration of hydrogen into the outer recirculation zone as shown in Figure 6.

Similarly, the influence of varying the air feed panel hydraulic diameter on the NO_x characteristics is shown in Figure 15. From Figure 15 with an increase in air feed hydraulic diameter and the associated increase in momentum flux ratio and hence the mixing characteristics, there is a net improvement in the predicted NO_x formation. This can be related to the jet-in-crossflow momentum flux ratio and to the recirculation zone that surrounds and stabilises the H_2 flames. An increase in the cross flow momentum flux ratio results in a greater penetration depth as shown in Equation 4. Upon further increasing the momentum flux ration beyond a critical value, the H_2 stream penetrates the shear layer between the cross-flow streams and consequently increases the NO_x emissions.

Copyright © 2019 ASME

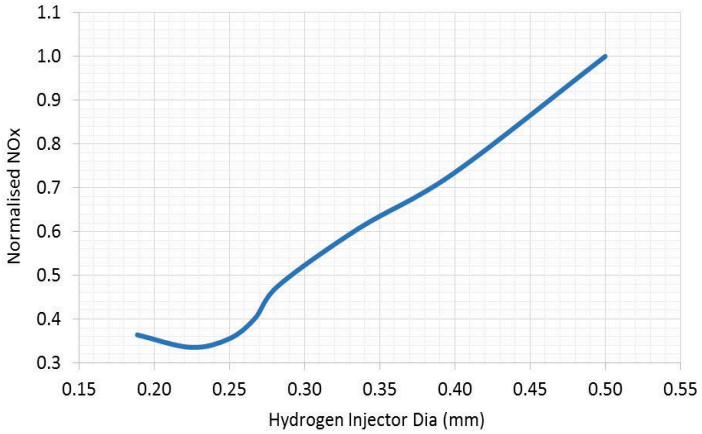


Figure 14- Normalised NO_x vs the Hydrogen Injector Diameter

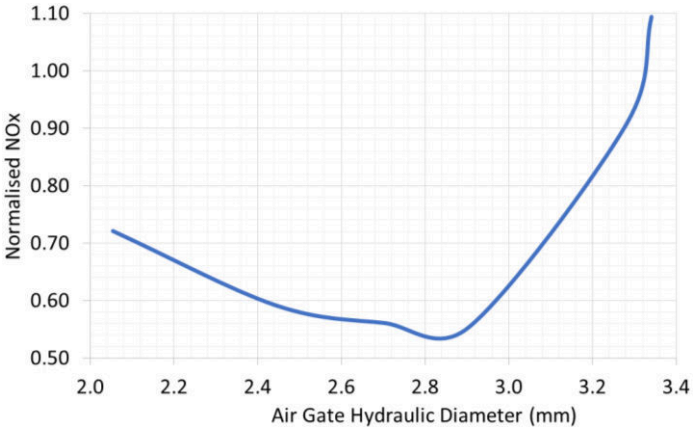
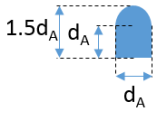
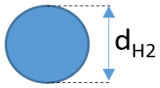


Figure 15- Normalised NO_x vs the Air Feed Hydraulic Diameter

The temperature and NO_x contour plots along the mid-section of the computational domain for the best and the worst case scenarios are shown in Figure 16 and Figure 17. The dimensions of the "preferred injector" are shown in Table 4. The calculated NO_x shown in Figure 17, reflects the flame structure shown in Figure 16. The low momentum flux ratio results in reduced penetration of the hydrogen into the oxidiser stream. This results in a greater amount of heat release occurring at the lower side of the flame as shown in Figure 16. However, increasing the momentum flux ratio between the jet streams results in more penetration of the fuel into the oxidiser stream. This results in the heat release occurring in the shear layers between the outer and inner recirculation zones. This is shown as in Figure 16. The flame zone length is also reduced, which further results in decreased peak temperature regions and hence reduced NO_x formation regions as shown in Figure 17.

From Figure 16 it is observed that the anchoring position of the hydrogen flame has been impacted because of the variation in the air feed hydraulic diameter and the hydrogen inlet diameter. Upon increasing the momentum flux ratio, the distance between the recirculation zone and the injected H_2 jet is reduced. If the distance becomes too marginal, the anchoring position of the hydrogen flame is altered. The flame anchors onto the shear layer of the air feed panel recirculation zone instead of the mixing segment of the burner [63]. The can therefore possibly have implications on the stability of the flame [59] [61].

Table 4- Preferred Injector Geometry

	Shape	Hydraulic Diameter (mm)	Aspect Ratio
Air Feed Panel		1.828	1.5
Hydrogen Inlet Diameter		0.30	1

It must also be emphasized that the peak NO_x values predicted for all the injector cases are higher than those investigated in the literature [8] [17]. The previous analyses carried out on micromix combustion systems have been limited to its application in low power systems. However, the current investigation is carried out for the implementation of the micromix combustion technology for high thrust class engines hence an increase in heat release per injector. Due to this increase in heat release per injector the mass flow rates for both the fuel and the oxidiser have increased which further leads to thicker and longer micromix flames and hence greater NO_x emissions.

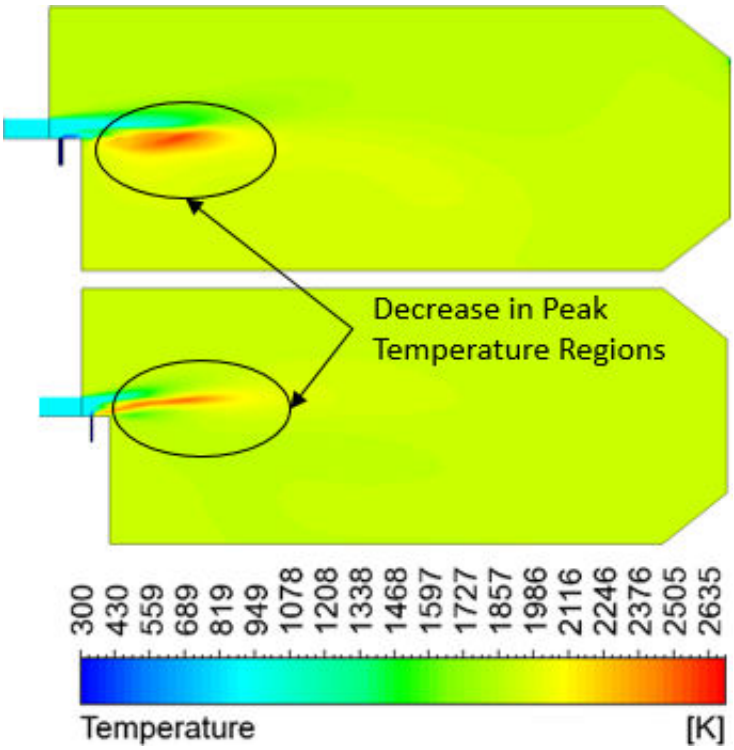


Figure 16- Total Temperature Comparison: D1 and D22

Copyright © 2019 ASME

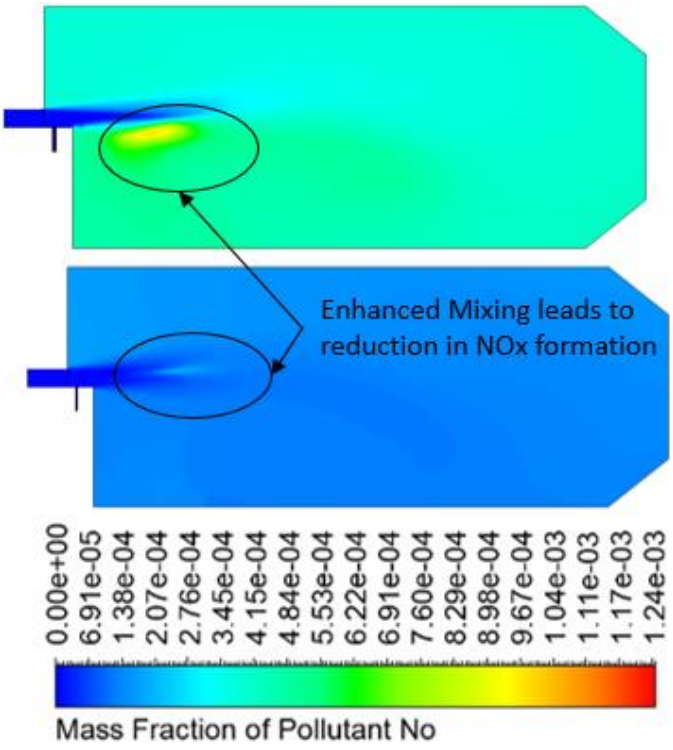


Figure 17- NO_x fraction distribution: D1 and D22

LIMITATIONS OF THE STUDY

The current analysis gives us a useful insight into the micromix flame characteristics. Nevertheless, the authors do well recognise the various limitations associated with the current study.

"One-variable-at-a-time" parametric analysis was carried out to understand the influence of varying one geometrical variable at a given time. The primary disadvantages associated with carrying out such an analysis are its limitations in predicting the interaction of multiple design variables in the design space. The result obtained for this study, however, may be used to guide the design space to be explored as a part of a future DOE analysis.

A RANS based CFD approach has been used for the analysis. RANS simulations cannot represent the transient nature of the velocity and the turbulent fluctuations in the flow. These fluctuations affect the predicted species, the temperatures in the reactive flow field and hence the emission predictions.

The effect of the Lewis number is apparent from the constant flame temperature, along with the flame surface predicted by all the numerical simulations shown in this paper. According to the laminar flame theory when a diffusion flame is stretched, the flame temperature drops due to the increased reactant fluxes and the Damkohler number effects. Damkholer number is defined as the ratio of the diffusion mixing time to the chemical reaction time and it reflects the completeness of the chemical reactions. As the flame is stretched the residence time of the reactants in the reaction zone decreases and the chemical reactions are more incomplete, therefore the flame temperature consequently decreases [54]. Studies carried out by [48] indicate that the preferential diffusion resulting from non-unity Lewis number has a strong influence on the flame temperature. For lighter species this effect is even more profound, therefore the flame temperatures are expected to be lower in a hydrogen diffusion flames. The current analysis is limited to steady-state flows, although these effects become even more profound if the unsteadiness of the flame is considered. Considerable research efforts have been placed on how the coupled effect of flame unsteadiness, curvature, stretch, and Lewis number affect the diffusion flames [57-59]. All of these studies indicate that the local flame temperature can depart considerably from the temperature distribution measured for a steady state flame. Hence the Lewis number effects will be accounted for in the FGM library for future numerical simulations; as well as, using LES to better capture the unsteady mixing effects.

CONCLUSION

The results of the numerical simulations of the test burner show the expected recirculation zones and reactive flow fields, which are an important key driver for the micromix combustion phenomenon.

The first part of the study highlights the importance of down-selecting the suitable hydrogen-air combustion chemistry mechanism. Significant variations in the reactive flow-field were observed with the variations in the H_2/air combustion chemistry mechanisms. This establishes the relevance of selecting a suitable combustion chemistry mechanism for reactive flow analysis.

For the second part of the study, a parametric analysis carried out for the micromix burner segment revealed that it is well possible to positively influence the flame shape by altering the recirculation zones. The adequate selection of the burner design parameters allows us to adjust the flame length, and the inter-shear layer formed between the recirculation zones. This allows the suppression of NO_x rich regions formed in the post shear layer zone. A decrease in NO_x emission by more than 60% was observed, just by varying two design parameters. That stated the micromix combustor does hold greater potential for further NO_x reduction. The influence of the hydrogen mixing distance and the hydrogen-air offset distance on the micromix combustion characteristics require further investigation. Consequently, a detailed DOE analysis will be carried out in future work.

The paper presents some of the initial numerical analysis undertaken to explore the micromix combustion design space and the associated reacting flow field. The design limitations, the reactive flow field phenomenon and the modelling challenges associated with the design of a micromix combustion system are identified and stated. This analysis will help guide the on-going/future more detailed numerical and experimental work at Cranfield. The limitations identified will be fully addressed and expanded upon in the detailed numerical and experimental future work.

ACKNOWLEDGEMENTS

This project has received funding from the European Union's Horizon 2020 research and innovation programme under grant agreement No 769241.

Copyright © 2019 ASME

REFERENCES

[1] Braun-Unkhoff, M. and Riedel, U. (2014). Alternative fuels in aviation. *CEAS Aeronautical Journal*, 6(1), pp.83-93.

[2] International Air Transport Association (IATA). http://www.iata.org/pressroom/facts_figures/factsheets/Pages/environment.aspx (2011)

[3] Intergovernmental Panel on Climate Change (IPPC), Fourth Assessment Report, "Climate Change 2007: Mitigation of Climate Change". http://www.ipcc.ch/publications_and_data/publications_ipcc_fourth_assessment_report_wg3_report_mitigation_of_climate_change.htm (2007)

[4] "Flightpath 2050 Europe's vision for the Aviation Report" https://ec.europa.eu/transport/sites/transport/files/modes/air/ doc/flightpath2050.pdf

[5] Klug, H.G., "The Cryoplane Project – Aircraft Using Cryogenic Fuel and Their Impact on the Atmosphere", XVIII General Assembly, European Geophysical Society, 1993

[6] Khandelwal, B., Karakurt, A., Sekaran, P., Sethi, V. and Singh, R. (2013). Hydrogen powered aircraft: The future of air transport. *Progress in Aerospace Sciences*, 60, pp.45-59.

[7] Brand, J., Sampath, S., Shum, F., Bayt, R. and Cohen, J. (2003). Potential Use of Hydrogen In Air Propulsion. In: *AIAA International Air and Space Symposium and Exposition: The Next 100 Years, International Air and Space Symposium (Evolution of Flight)*. [online] AIAA. Available at: https://doi.org/10.2514/6.2003-2879

[8] DAHL, G. (1998). Engine control and low-NOx combustion for hydrogen fuelled aircraft gas turbines. *International Journal of Hydrogen Energy*, 23(8), pp.695-704.

[9] Murthy. P., 2011. "Numerical study of H_2 micro-mix combustors for aero gas turbine engines". MSc thesis, Cranfield University

[10] Karakurt, A., 2013. "Parametric investigation of combustion characteristics of an H_2 micromix combustor concept". MSc thesis, Cranfield University

[11] Degroote, A., 2013. "Assessment of the feasibility of controlling the outlet temperature distribution of a novel micromix combustor". MSc thesis, Cranfield University

[12] Asanitthong, S., 2014. "Outlet temperature distribution control and heat transfer calculation for an H_2 micromix combustor". MSc thesis, Cranfield University

[13] Bantel, M.P., 2014. "Comparison study of combustion models for a conceptual hydrogen micromix combustor". MSc thesis, Cranfield University

[14] Sabin, R., 2016. "Comparative performance study of CFD species transport models for H_2 micromix combustion". MSc thesis, Cranfield University

[15] Ben Abdallah, R., Sethi, V., Gauthier, P., Rolt, A. and Abbott, D. (2018). A Detailed Analytical Study of Hydrogen Reaction in a Novel Micromix Combustion System.

[16] Zeldovich, Y.B., The Oxidation of Nitrogen in Combustion and Explosions. Acta Physicochimica URSS 21, pp. 577-628, 1946

[17] Ayed, A., Kusterer, K., Funke, H., Keinz, J. and Bohn, D. (2017). CFD based exploration of the dry-low-NO x hydrogen micromix combustion technology at increased energy densities. *Propulsion and Power Research*, 6(1), pp.15-24.

[18] Davies, T. and Beér, J. (1971). Flow in the wake of bluff-body flame stabilizers. Symposium (International) on Combustion, 13(1), pp.631-638.

[19] CORDIS | European Commission. (2018). ENABLing cryogEnic Hydrogen based CO2 free air transport (ENABLEH2) | Projects | H2020 | CORDIS | European Commission. [online] Available at: <https://cordis.europa.eu/project/rcn/216008_en.html>

[20] Ultimate.aero. (2018). Ultimate PROJECT - Objectives. [online] Available at: http://www.ultimate.aero/page/en/about/objectives.php

[21] Ayed, A., Kusterer, K., Funke, H., Keinz, J. and Bohn, D. (2017). CFD based exploration of the dry-low-NO x hydrogen micromix combustion technology at increased energy densities. Propulsion and Power Research, 6(1), pp.15-24.

[22] Menter, F.R., "Two-equation eddy-viscosity turbulence models for engineering applications", AIAA-Journal., 32(8), pp. 1598 - 1605, 1994.

[23] Pitsch, H., Chen, M. and Peters, N. (1998). Unsteady flamelet modelling of turbulent hydrogen-air diffusion flames. Symposium (International) on Combustion, 27(1), pp.1057-1064.

[24] Nakod, P., Yadav, R., Rajeshirke, P. and Orsino, S. (2014). A Comparative Computational Fluid Dynamics Study on Flamelet-Generated Manifold and Steady Laminar Flamelet Modeling for Turbulent Flames. Journal of Engineering for Gas Turbines and Power, 136(8), p.081504.

[25] Van Oijen, J. and de Goey, L. (2002). Modelling of premixed counterflow flames using the flamelet-generated manifold method. Combustion Theory and Modelling, 6(3), pp.463-478.

[26] Vreman, A., van Oijen, J., de Goey, L. and Bastiaans, R. (2009). Direct numerical simulation of hydrogen addition in turbulent premixed Bunsen flames using flamelet-generated manifold reduction. International Journal of Hydrogen Energy, 34(6), pp.2778-2788.

[27] Bastiaans, R., van Oijen, J. and de Goey, L. (2006). Application of Flamelet-Generated Manifolds and Flamelet Analysis of Turbulent Combustion International Journal for Multiscale Computational Engineering, 4(3), pp.307-317.

[28] Olm, C., Zsély, I., Pálvölgyi, R., Varga, T., Nagy, T., Curran, H. and Turányi, T. (2014). Comparison of the performance of several recent hydrogen combustion mechanisms. Combustion and Flame, 161(9), pp.2219-2234.

[29] Babazzi, G., 2018. "Turbulence-Chemistry Interaction Study for a Hydrogen Micromix Combustion System". MSc thesis, Cranfield University

[30] Kéromnès, A., Metcalfe, W., Heufer, K., Donohoe, N., Das, A., Sung, C., Herzler, J., Naumann, C., Griebel, P., Mathieu, O., Krejci, M., Petersen, E., Pitz, W. and Curran, H. (2013). An experimental and detailed chemical kinetic modeling study of hydrogen and syngas mixture oxidation at elevated pressures. *Combustion and Flame*, 160(6), pp.995-1011.

Copyright © 2019 ASME

[31] Healy, D., Kalitan, D., Aul, C., Petersen, E., Bourque, G. and Curran, H. (2010). Oxidation of C1−C5 Alkane Quinternary Natural Gas Mixtures at High Pressures. *Energy & Fuels*, 24(3), pp.1521-1528.

[32] Ó Conaire, M., Curran, H., Simmie, J., Pitz, W. and Westbrook, C. (2004). A comprehensive modeling study of hydrogen oxidation. *International Journal of Chemical Kinetics*, 36(11), pp.603-622.

[33] Konnov, A. (2008). Remaining uncertainties in the kinetic mechanism of hydrogen combustion. *Combustion and Flame*, 152(4), pp.507-528.

[34] Li, J., Zhao, Z., Kazakov, A., Chaos, M., Dryer, F. and Scire, J. (2007). A comprehensive kinetic mechanism for CO, CH2O, and CH3OH combustion. *International Journal of Chemical Kinetics*, 39(3), pp.109-136.

[35] Hong, Z., Davidson, D. and Hanson, R. (2011). An improved H2/O2 mechanism based on recent shock tube/laser absorption measurements. *Combustion and Flame*, 158(4), pp.633-644.

[36] Burke, M., Chaos, M., Ju, Y., Dryer, F. and Klippenstein, S. (2011). Comprehensive H2/O2 kinetic model for high-pressure combustion. *International Journal of Chemical Kinetics*, 44(7), pp.444-474.

[37] Saxena, P. and Williams, F. (2006). Testing a small detailed chemical-kinetic mechanism for the combustion of hydrogen and carbon monoxide. *Combustion and Flame*, 145(1-2), pp.316-323.

[38] Davis, S., Joshi, A., Wang, H. and Egolfopoulos, F. (2005). An optimized kinetic model of H2/CO combustion. *Proceedings of the Combustion Institute*, 30(1), pp.1283-1292.

[39] Starik, A., Titova, N., Sharipov, A. and Kozlov, V. (2010). Syngas Oxidation Mechanism. *Combustion, Explosion, and Shock Waves*, 46(5), pp.491-506.

[40] H. Wang, X. You, A.V. Joshi, S.G. Davis, A. Laskin, F. Egolfopoulos, C.K. Law, USC Mech Version II. High-temperature Combustion Reaction Model of H_2/CO/C_1–C_4 Compounds.

[41] CRECK modelling Group, Hydrogen/CO Mechanism Version 1201. <http://creckmodeling.chem.polimi.it/kinetic.html/>.

[42] Mechanical and Aerospace Engineering (Combustion Research), University of California at San Diego: Chemical-Kinetic Mechanisms for Combustion Applications, San Diego Mechanism, version 2011-11-22.<http://combustion.ucsd.edu/>.

[43] G.P. Smith, D.M. Golden, M. Frenklach, N.W. Moriary, B. Eiteneer, M. Goldenberg, C.T. Bowman, R.K. Hanson, S. Song, W.C. Gardiner, V.V. Lissianski, Z. Qin, GRI-Mech 3.0. <http://www.me.berkeley.edu/gri_mech/>.

[44] Sun, H., Yang, S., Jomaas, G. and Law, C. (2007). High-pressure laminar flame speeds and kinetic modeling of carbon monoxide/hydrogen combustion. *Proceedings of the Combustion Institute*, 31(1), pp.439-446.

[45] Gimenez-Lopez, J., Rasmussen, C., Hashemi, H., Alzueta, M., Gao, Y., Marshall, P., Goldsmith, C. and Glarborg, P. (2016). Experimental and Kinetic Modeling Study of C2H2Oxidation at High Pressure. *International Journal of Chemical Kinetics*, 48(11), pp.724-738.

[46] Ahmed, S., Mauß, F., Moréac, G. and Zeuch, T. (2007). A comprehensive and compact n-heptane oxidation model derived using chemical lumping. *Phys. Chem. Chem. Phys.*, 9(9), pp.1107-1126.

[47] Zsély, I., Zádor, J. and Turányi, T. (2005). Uncertainty analysis of updated hydrogen and carbon monoxide oxidation mechanisms. *Proceedings of the Combustion Institute*, 30(1), pp.1273-1281.

[48] Dagaut, P., Lecomte, F., Mieritz, J. and Glarborg, P. (2003). Experimental and kinetic modeling study of the effect of NO and SO2 on the oxidation of CO? H2 mixtures. *International Journal of Chemical Kinetics*, 35(11), pp.564-575.

[49] Kazakov. A, and Frenklach. M, http://www.me.berkeley.edu/drm/

[50] Reaction Design: San Diego, 2015. ANSYS Chemkin Theory Manual 17.0 (15151).

[51] Law, C. (2011). Combustion physics. Cambridge [etc.]: Cambridge University Press.

[52] Goswami M, Volkov E.N., Konnov A.A, Updated Kinetics Mechanism for NOx Prediction and Hydrogen Combustion, Technical Report TU Eindhoven

[53] Hwang, S., Ryu, S., Witt, K. and Rabinowitz, M. (2005). High temperature rate coefficient measurements of H+O2 chain-branching and chain-terminating reaction. *Chemical Physics Letters*, 408(1-3), pp.107-111.

[54] Ansys, 2014, Ansys Theory Guide release 18 ed.

[55] Ishizuka, S. (1982). An experimental study on the opening of laminar diffusion flame tips. *Symposium (International) on Combustion*, 19(1), pp.319-326.

[56] Cuenot, B. and Poinsot, T. (1994). Effects of curvature and unsteadiness in diffusion flames. Implications for turbulent diffusion combustion. *Symposium (International) on Combustion*, 25(1), pp.1383-1390.

[57] Hancock, R., Schauer, F., Lucht, R., Katta, V. and Hsu, K. (1996). Thermal diffusion effects and vortex-flame interactions in hydrogen jet diffusion flames. *Symposium (International) on Combustion*, 26(1), pp.1087-1093.

[58] Katta, V. and Roquemore, W. (1995). On the structure of a stretched/compressed laminar flamelet—Influence of preferential diffusion. *Combustion and Flame*, 100(1-2), pp.61-70.

[59] Wang, P., Hu, S. and Pitz, R. (2007). Numerical investigation of the curvature effects on diffusion flames. *Proceedings of the Combustion Institute*, 31(1), pp.989-996.

[60] Gauthier P.Q. (2017). Comparison of Temperature Fields and Emissions Predictions Using Both an FGM Combustion Model, With Detailed Chemistry, and a Simple Eddy Dissipation Combustion Model With Simple Global Chemistry. *ASME. Turbo Expo: Power for Land, Sea, and Air, Volume 4B: Combustion, Fuels and Emissions* ():V04BT04A068.

[61] Funke, H., Keinz, J., Kusterer, K., Ayed, A., Kazari, M., Kitajima, J., Horikawa, A. and Okada, K. (2016). Experimental and Numerical Study on Optimizing the Dry Low NOx Micromix Hydrogen Combustion Principle for

Copyright © 2019 ASME

Industrial Gas Turbine Applications. Journal of Thermal Science and Engineering Applications, 9(2), p.021001.

[62] Ayed, A., Kusterer, K., Funke, H., Keinz, J. and Bohn, D. (2017). CFD based exploration of the dry-low-NO x hydrogen micromix combustion technology at increased energy densities. *Propulsion and Power Research*, 6(1), pp.15-24.

[63] Funke, H., Keinz, J., Kusterer, K., Ayed, A., Kazari, M., Kitajima, J., Horikawa, A. and Okada, K. (2016). Experimental and Numerical Study on Optimizing the Dry Low NOx Micromix Hydrogen Combustion Principle for Industrial Gas Turbine Applications. Journal of Thermal Science and Engineering Applications, 9(2), p.021001.

Copyright © 2019 ASME



https://dspace.org/

Injector design space exploration for an ultra-low NOx hydrogen micromix combustion system

Agarwal, Parash; Sun, Xiaoxiao; Gauthier, Pierre Q.; Sethi, Vishal

2019-11-05
ASME
https://doi.org/10.1115/GT2019-90833
Agarwal P, Sun X, Gauthier PQ, Sethi V. (2019) Injector design space exploration for an ultra-low NOx hydrogen micromix combustion system. In: ASME Turbo Expo 2019: Turbomachinery Technical Conference and Exposition, 17-21 June 2019, Phoenix, Arizona, Paper number GT2019-90833

Downloaded from a DSpace repository. https://dspace.org/